



STABILITY ANALYSIS OF HYDROMAGNETIC INVISCID INCOMPRESSIBLE STRATIFIED PARALLEL LINEAR SHEAR FLOW

K.Sumathi and R.Panneerselvi

Department of Mathematics, PSGR Krishnammal College for women,
Coimbatore, Tamilnadu, India

T.Arunachalam

2Department of Mathematics, Kumaraguru College of Technology,
Coimbatore, Tamil Nadu, India

ABSTRACT

The linear stability of an inviscid, incompressible plane-parallel magnetohydrodynamic stratified shear flow with velocity $\vec{U} = (U(z), 0, 0)$ and a constant magnetic field confined between two horizontal parallel plates is analyzed. The governing equations with suitable boundary conditions are solved using normal mode approach. Approximate analytical solutions are found to determine the growth rate. The effects of various non-dimensional parameters like Brunt-vaisala frequency (N), Magnetic Pressure Number (S), Magnetic Reynolds Number (Rm) and Richardson Number (Ri) with respect to wave number is shown graphically.

Keywords: stratification, normal-mode analysis, Magnetic Reynolds number, eigen values, method of small oscillation

Cite this Article: K.Sumathi, T.Arunachalam and R.Panneerselvi, Stability Analysis of Hydromagnetic Inviscid Incompressible Stratified Parallel Linear Shear Flow, International Journal of Mechanical Engineering and Technology, 9(5), 2018, pp. 556–570.

<http://iaeme.com/Home/issue/IJMET?Volume=9&Issue=5>

1. INTRODUCTION

The linear stability of a stratified shear flow of an inviscid, incompressible fluid has been extensively studied by many authors. The standard method for obtaining stability criteria from the linearized equations for an inviscid incompressible fluid in a plane parallel flow is normal-mode analysis, which leads to the Rayleigh stability equation (Drazin and Reid [5], Drazin and Howard [6]). The normal-mode stability of plane parallel flows of an inviscid, incompressible stratified fluid has been analyzed by Taylor [16] and Goldstein [7].

Drazin [6] discussed the stability of parallel flow in a parallel magnetic field at small magnetic Reynolds number. Kent ([9], [10]) studied the effect of varying magnetic field on the stability of parallel flows. Agarwal and Agarwal [1] analyzed the stability of heterogeneous shear flow in the presence of parallel magnetic field. Kochar and Jain [11] and Rathy and Harikishan [14] have also discussed the same problem. Small perturbations of a parallel shear flow in an inviscid, incompressible stably stratified fluid are studied by Collyer [3].

The Kuo's eigen value problem (Kuo [12]) governs the normal mode stability of barotropic zonal flows of an inviscid, incompressible fluid on a β - plane. Barston [2] has introduced a new method in the linear stability analysis of plane parallel flows of inviscid, incompressible homogeneous fluid. Stability of stratified shear flows in channels with variable cross section was studied by Reddy and Subbiah [15]. Linear stability of inviscid, parallel and stably stratified shear flow under the assumption of smooth strictly monotonic profiles of shear flow and density is studied by Hirota and Morrison [8].

In the present study, the work of Padmini and Subbiah [13] is extended to study the effect of uniform magnetic field. The stability of stratified shear flow of an inviscid, incompressible fluid confined between two rigid planes at $z = \pm L$ under the influence of uniform magnetic field is considered. The following analysis is based on the linear velocity profile with long wavelength approximations.

2. FORMULATION OF THE PROBLEM

Consider an electrically conducting stratified inviscid Boussinesq fluid flowing between two horizontal plates. A uniform magnetic field is applied. We use Cartesian coordinates (x, y, z) taking the mid-point between two parallel plates as origin. The plates are considered at a distance $2L$ apart. Under the above mentioned assumptions the schematic representation of the problem is given in Figure 1.

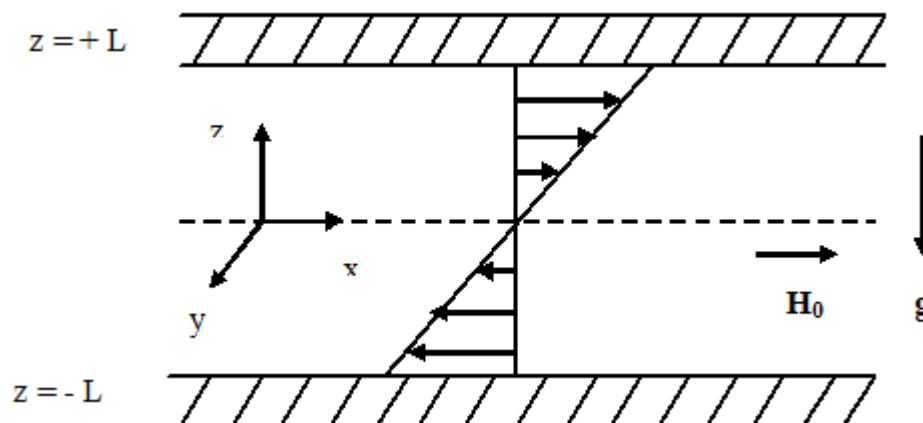


Figure 1 Schematic representation of the problem

With the Boussinesq's approximation, the governing equations for the motion of an inviscid, incompressible, stratified shear fluid confined between two horizontal infinite rigid planes under horizontal magnetic field are

$$\nabla \cdot \vec{q} = 0 \tag{1}$$

$$\frac{\partial \vec{q}}{\partial t} + (\vec{q} \cdot \nabla) \vec{q} = \frac{-\nabla p}{\rho_0} - \frac{\rho g z}{\rho_0} + \mu_m (\nabla \times \vec{H}) \times \vec{H} \tag{2}$$

$$\frac{\partial \rho}{\partial t} + (\vec{q} \cdot \nabla) \rho = 0 \tag{3}$$

$$\frac{\partial \vec{H}}{\partial t} = \eta \nabla^2 \vec{H} + \nabla \times (\vec{q} \times \vec{H}) \quad (4)$$

$$\nabla \cdot \vec{H} = 0 \quad (5)$$

where \vec{q} , ρ , p , g , η , μ_m and \vec{H} denote the velocity, density, pressure, acceleration due to gravity, resistivity, magnetic permeability and the magnetic field respectively.

If the fluid is confined between two horizontal rigid planes at $z = \pm L$, the boundary conditions are

$$\vec{q} = 0 \quad \text{at } z = \pm L \quad (6)$$

The equilibrium state is given by

$$-\frac{\partial p_e}{\partial z} - \rho_e g = 0 \quad (7)$$

The dimensionless forms have been rendered for the quantities with respect to the characteristic length (L) and the characteristic velocity (U_0) as the following:

$$t = \frac{Lt^*}{U_0}, \quad p = \rho_0 U_0^2 p^*, \quad \rho = \frac{\rho_0 U_0^2 N_0^2}{Lg} \rho^*, \quad \vec{H} = H_0 \vec{H}^* \quad \text{and } (x,y,z) = L(x^*,y^*,z^*) \quad (8)$$

where $N^2 = -\frac{g}{\rho_0} \left(\frac{d\rho}{dz}\right)$ is the Brunt-Vaisala frequency which is assumed to be positive for static stability and N_0^2 is a typical value of Brunt-Vaisala frequency in the flow domain. Substitute the above dimensionless quantities in the governing equations, equations (1) - (5) reduce to (on removing asterisks)

$$\nabla \cdot \vec{q} = 0 \quad (9)$$

$$\frac{\partial \vec{q}}{\partial t} + (\vec{q} \cdot \nabla) \vec{q} = -\nabla p - Ri \, g \hat{k} + S(\nabla \times \vec{H}) \times \vec{H} \quad (10)$$

$$\frac{\partial \rho}{\partial t} + (\vec{q} \cdot \nabla) \rho = 0 \quad (11)$$

$$\frac{\partial \vec{H}}{\partial t} = \frac{1}{Rm} \nabla^2 \vec{H} + \nabla \times (\vec{q} \times \vec{H}) \quad (12)$$

$$\nabla \cdot \vec{H} = 0 \quad (13)$$

where, $S = \frac{\mu_m H_0^2}{\rho U_0^2}$, Magnetic Pressure Number

$Rm = \frac{LU_0}{\eta}$, Magnetic Reynolds Number

$Ri = \frac{g\beta L^2}{\rho_0 U_0^2}$, Richardson Number

The boundary condition in non-dimensional form is

$$\vec{q} = 0 \quad \text{on } z = \pm 1 \quad (14)$$

Decomposing the flow into a basic state and a disturbance as $(U(z) + u, v, w)$, $\rho_e(z) + \rho$, $p_e(z) + p$ and $(H_0 + h_x, h_y, h_z)$, the basic state $U(z), \rho_e, p_e, H_0$ are governed by the equations above.

The linearized perturbation equations for infinitesimal normal modes of the form $f(z)e^{ik(x+ly-\sigma t)}$, (k and l are the horizontal and transverse wave number and σ the complex wave velocity) are obtained as

$$ik(u + lv) + \frac{\partial w}{\partial z} = 0$$

$$ik(U - \sigma)u + w \frac{\partial U}{\partial z} = -ik(p + H_0 S(h_y - lh_x))$$

$$ik(U - \sigma)v = -ik(p - H_0 S(h_y - lh_x))$$

$$\begin{aligned}
 ik(U - \sigma)w &= -\frac{\partial p}{\partial z} - Ri \rho + H_0 S \left(ik(1 + l)h_z - \frac{\partial h_y}{\partial z} - \frac{\partial h_x}{\partial z} \right) \\
 ik(U - \sigma)\rho - \frac{N^2}{N_0^2} w &= 0 \\
 ik(h_x + lh_y) + \frac{\partial h_z}{\partial z} &= 0 \\
 \left(-ik\sigma - \frac{1}{Rm} \left(-k^2(1 + l^2) + \frac{\partial^2}{\partial y^2} \right) \right) h_x &= ikl(H_0 u + Uh_y - H_0 v) - H_0 \frac{\partial w}{\partial z} + \frac{\partial}{\partial z} (Uh_z) \\
 \left(-ik\sigma - \frac{1}{Rm} \left(-k^2(1 + l^2) + \frac{\partial^2}{\partial y^2} \right) \right) h_y &= -ik(H_0 u + Uh_y - H_0 v) - H_0 \frac{\partial w}{\partial z} \\
 \left(-ik\sigma - \frac{1}{Rm} \left(-k^2(1 + l^2) + \frac{\partial^2}{\partial y^2} \right) \right) h_z &= ik((1 + l)H_0 w - Uh_z) \tag{15}
 \end{aligned}$$

The associated boundary conditions are

$$u = v = w = 0 \quad \text{on } z = \pm 1 \tag{16}$$

3. EIGEN VALUES AND EIGEN FUNCTIONS FOR LONG WAVES

Here, we consider the analysis for long wave approximation (i.e) k is assumed to be small and the flow is assumed to be bounded between two plates $z = \pm 1$. In order to get closed form solutions, we consider the linear velocity profile as the basic flow $U(z) = z$.

Hence equation (15) reduces to the form

$$\begin{aligned}
 ik(u + lv) + \frac{\partial w}{\partial z} &= 0 \\
 ik(-\sigma + z)u + w &= -ik(p + H_0 S(h_y - lh_x)) \\
 ik(-\sigma + z)v &= -ik(p - H_0 S(h_y - lh_x)) \\
 ik(-\sigma + z)w &= -\frac{\partial p}{\partial z} - Ri \rho + H_0 S \left(ik(1 + l)h_z - \frac{\partial h_y}{\partial z} - \frac{\partial h_x}{\partial z} \right) \\
 ik(-\sigma + z)\rho - \frac{N^2}{N_0^2} w &= 0 \\
 ik(h_x + lh_y) + \frac{\partial h_z}{\partial z} &= 0 \\
 \left(-ik\sigma - \frac{1}{Rm} \left(-k^2(1 + l^2) + \frac{\partial^2}{\partial y^2} \right) \right) h_x &= ikl(H_0 u + zh_y - H_0 v) - H_0 \frac{\partial w}{\partial z} + \frac{\partial}{\partial z} (zh_z) \\
 \left(-ik\sigma - \frac{1}{Rm} \left(-k^2(1 + l^2) + \frac{\partial^2}{\partial y^2} \right) \right) h_y &= -ik(H_0 u + zh_y - H_0 v) - H_0 \frac{\partial w}{\partial z} \\
 \left(-ik\sigma - \frac{1}{Rm} \left(-k^2(1 + l^2) + \frac{\partial^2}{\partial y^2} \right) \right) h_z &= ik((1 + l)H_0 w - zh_z) \tag{17}
 \end{aligned}$$

We assume the series expansions with respect to the wave number k in the form

$$f = f_0 + kf_1 + k^2 f_2 + \tag{18}$$

where, $f = (u, v, w, \sigma, \rho, h_x, h_y, h_z)$

Substituting equation (18) into equation (17) and equating the coefficients of same degree terms and neglecting k^2 we get the following set of differential equations:

Zeroth order equations:

$$\begin{aligned}
 iu_0 + ilv_0 + \frac{\partial w_0}{\partial z} &= 0 \\
 iT(z)u_0 + w_0 &= -ip_0 \\
 iT(z)v_0 &= -ilp_0
 \end{aligned}$$

$$\begin{aligned}
 -\frac{\partial p_0}{\partial z} - Ri \rho_0 &= 0 \\
 iT(z)\rho_0 - \frac{N^2}{N_0^2}v_0 &= 0
 \end{aligned} \tag{19}$$

$$\begin{aligned}
 ih_{x0} + ilh_{y0} + \frac{\partial h_{z0}}{\partial z} &= 0 \\
 -\frac{1}{Rm} \left(\frac{\partial^2 h_{x0}}{\partial z^2} \right) &= i(1+l)H_0u_0 \\
 -\frac{1}{Rm} \left(\frac{\partial^2 h_{y0}}{\partial z^2} \right) &= i(1+l)H_0v_0 \\
 -\frac{1}{Rm} \left(\frac{\partial^2 h_{z0}}{\partial z^2} \right) &= i(1+l)H_0w_0
 \end{aligned} \tag{20}$$

where $T(z) = z - \sigma_0$

First order equations:

$$\begin{aligned}
 iu_1 + ilv_1 + \frac{\partial w_1}{\partial z} &= 0 \\
 iT(z)u_1 + w_1 - i\sigma_1u_0 &= -ip_1 - iH_0S(h_{y0} - lh_{x0}) \\
 iT(z)v_1 - i\sigma_1v_0 &= -ilp_1 + iH_0S(h_{y0} - lh_{x0}) \\
 \frac{\partial p_1}{\partial z} + Ri \rho_1 &= -H_0S \left(\frac{\partial h_{x0}}{\partial z} + \frac{\partial h_{y0}}{\partial z} \right) \\
 iT(z)w_1 - i\sigma_1w_0 &= -ilp_1 - Slh_{x0}(1+l) \\
 iT(z)\rho_1 - i\sigma_1\rho_0 - \frac{N^2}{N_0^2}w_1 &= 0
 \end{aligned} \tag{21}$$

$$\begin{aligned}
 ih_{x1} + ilh_{y1} + \frac{\partial h_{z1}}{\partial z} &= 0 \\
 -\frac{1}{Rm} \left(\frac{\partial^2 h_{x1}}{\partial z^2} \right) &= i(1+l)u_1H_0 - iT(z)h_{x0} + h_{z0} \\
 -\frac{1}{Rm} \left(\frac{\partial^2 h_{y1}}{\partial z^2} \right) &= i(1+l)v_1H_0 - iT(z)h_{y0} \\
 -\frac{1}{Rm} \left(\frac{\partial^2 h_{z1}}{\partial z^2} \right) &= i(1+l)w_1H_0 - iT(z)h_{z0}
 \end{aligned} \tag{22}$$

The boundary conditions (16) reduces to

$$u_0 = u_1 = 0, \quad v_0 = v_1 = 0, \quad w_0 = w_1 = 0 \tag{23}$$

By simplifying equation (19) interms of w_0 , we get

$$T(z)^2 \frac{\partial^2 w_0}{\partial z^2} + \frac{Ri N^2}{N_0^2} (1+l^2)w_0 = 0 \tag{24}$$

The solution of Equation (24) is given by

$$w_0 = \begin{cases} A T(z)^{m_1} + B T(z)^{m_2}, & \lambda > 0 \\ T(z)^{\frac{1}{2}}(C + D \log(T(z))), & \lambda = 0 \\ T(z)^{\frac{1}{2}} \left(E \cos(k \log(T(z))) + F \sin(k \log(T(z))) \right), & \lambda < 0 \end{cases}$$

where $m_{1,2} = \frac{1 \pm \sqrt{\lambda}}{2}$, $\lambda = 1 - 4 Ri \frac{N^2}{N_0^2} (1+l^2)$, $k = \frac{\sqrt{-\lambda}}{2}$, A, B, C, D, E and F are arbitrary constants.

By applying the boundary conditions that the velocity should vanish at the boundaries (i.e) $w_0 = 0$ at $z = \pm 1$, we obtain the value of σ_0 as

$$\sigma_0 = \begin{cases} \frac{1+e^{\frac{2n\pi i}{m_1-m_2}}}{1-e^{\frac{2n\pi i}{m_1-m_2}}}, & \lambda \geq 0 \\ \frac{1+e^{\frac{n\pi}{k}}}{1-e^{\frac{n\pi}{k}}}, & \lambda < 0 \end{cases} \quad (25)$$

The solution of equations (19) and (20) can be obtained as

$$u_0 = \begin{cases} C_7 T(z)^{m_1-1} + C_8 T(z)^{m_2-1}, & \lambda \geq 0 \\ \frac{T(z)^{\frac{1}{2}}}{i} \left(\cos(k \log(T(z))) \left(\frac{E-kF}{1+l^2} - E \right) + \sin(k \log(T(z))) \left(\frac{kE+\frac{F}{2}}{1+l^2} - F \right) \right), & \lambda < 0 \end{cases}$$

$$v_0 = \begin{cases} C_5 T(z)^{m_1-1} + C_6 T(z)^{m_2-1}, & \lambda \geq 0 \\ \frac{-lT(z)^{-\frac{1}{2}}}{i(1+l^2)} \left(\cos(k \log(T(z))) \left(kF - \frac{E}{2} \right) + \sin(k \log(T(z))) \left(\frac{kE + \frac{F}{2}}{1+l^2} - F \right) \right), & \lambda < 0 \end{cases}$$

$$w_0 = \begin{cases} T(z)^{m_1} + BT(z)^{m_2}, & \lambda \geq 0 \\ T(z)^{\frac{1}{2}} \left(\cos(k \log(T(z))) + \sin(k \log(T(z))) \right), & \lambda < 0 \end{cases}$$

$$\rho_0 = \begin{cases} C_1 T(z)^{m_1-1} + C_2 T(z)^{m_2-1}, & \lambda \geq 0 \\ \frac{N^2 T(z)^{-\frac{1}{2}}}{iN_0^2} \left(\cos(k \log(T(z))) + F \sin(k \log(T(z))) \right), & \lambda < 0 \end{cases}$$

$$p_0 = \begin{cases} C_3 T(z)^{m_1} + C_4 T(z)^{m_2}, & \lambda \geq 0 \\ \frac{T(z)^{\frac{1}{2}}}{i(1+l^2)} \left(\cos(k \log(T(z))) \left(kF - \frac{1}{2} \right) + \sin(k \log(T(z))) \left(-k - \frac{F}{2} \right) \right), & \lambda < 0 \end{cases}$$

$$h_{x0} = Rm \begin{cases} C_{11} T(z)^{m_1+1} + C_{12} T(z)^{m_2+1}, & \lambda \geq 0 \\ T(z)^{\frac{3}{2}} \left(C_{44} \cos(k \log(T(z))) + C_{45} \sin(k \log(T(z))) \right), & \lambda < 0 \end{cases}$$

$$h_{y0} = Rm \begin{cases} C_{13} T(z)^{m_1+1} + C_{14} T(z)^{m_2+1}, & \lambda \geq 0 \\ T(z)^{\frac{3}{2}} \left(C_{42} \cos(k \log(T(z))) + C_{43} \sin(k \log(T(z))) \right), & \lambda < 0 \end{cases}$$

$$h_{z0} = Rm \begin{cases} C_9 T(z)^{m_1+2} + C_{10} T(z)^{m_2+2}, & \lambda \geq 0 \\ T(z)^{\frac{5}{2}} \left(C_{40} \cos(k \log(T(z))) + C_{41} \sin(k \log(T(z))) \right), & \lambda < 0 \end{cases}$$

Equation (21) is simplified in terms of w_1 as

$$T(z)^2 \frac{\partial^2 w_1}{\partial z^2} + \frac{Ri N^2}{N_0^2} (1+l^2) w_1 = \sigma_1 \left(T(z)^2 \frac{\partial^2 w_0}{\partial z^2} - Ri (1+l^2) i \rho_0 \right) - iH_0 S (1+l) T(z) \left(\frac{\partial h_{x0}}{\partial z} + \frac{\partial h_{y0}}{\partial z} \right) \quad (26)$$

The value of σ_1 can be obtained from the above equation by applying the boundary condition that $v_1(\pm 1) = 0$

$$\sigma_1 = \begin{cases} \frac{S Rm C_{39}}{Ri C_{37} - C_{38}}, & \lambda \geq 0 \\ \frac{-S Rm C_{62}}{C_{61}}, & \lambda < 0 \end{cases} \quad (27)$$

For the sake of brevity the constants are given in Appendix.

4. RESULTS AND DISCUSSION

In this work, we have presented the numerical results concerning linear stability of an inviscid, incompressible hydromagnetic stratified shear flow by considering the basic state velocity profile as linear. To determine the effects of the system parameters on the wave numbers, we plot the growth rate. Figures (2) – (11) depict the growth rate as a function of wave number and Magnetic Reynolds number for various parameters when $\lambda > 0$.

Figure. 2 shows the effect of Magnetic Reynolds number Rm on the growth rate. It shows that increase in Magnetic Reynolds number increases the growth rate with the increase in wave number thereby instability is triggered. Figure. 3 shows the effect of magnetic pressure number S on the growth rate. It is found that increasing magnetic pressure number leads to increase in the growth rate and have a destabilizing effect. The variation of growth rate with wave number is shown in Figure. 4 for various values of l . It is seen from Figure. 4 that increase in l increases the growth rate. It means that transverse wave number destabilize the flow against wave number.

In Figure. 5 the growth rate for various n is given. It shows that, there exists infinite number of modes for the given stability problem. In Figure. 6 we present the variation of growth rate with respect to wave number for different values of Ri . The result indicates that growth rate increases with Ri for unstable disturbances and for small Richardson number the flow becomes stable and as Richardson number increases the flow becomes unstable. Figure. 7 depicts the dependence of the growth rate on the Magnetic Reynolds number for various values of k when $Ri = 0.1$. From this, we conclude that with the increase in k the growth rate increases and leads to unstable disturbances.

The variation of growth rate with Rm for different values of l is displayed in Figure. 8. The result indicates that increase in l decreases the growth rate thereby destabilize the flow field. Figure. 9 shows the nature of growth rate with Rm for various values of Ri . It is understood from the figure that growth rate increases with the increase in Ri and results in unstable disturbances. Figure. 10 shows the graphs of the growth rates of the most unstable modes against the Magnetic Reynolds number (Rm). Figure. 11 portrays the growth rate as a function of Brunt-Vaisala frequency. It is noticed that increasing Brunt-Vaisala frequency stabilizes the system.

Figures (12) – (20) gives the idea about growth rate vs wave number, Magnetic Reynolds number and magnetic pressure number when $\lambda < 0$. The growth rate as a function of wave number is given in Figure.12 and Figure. 13 for several values of Rm . We can see from both the figures that the disturbances are stable for small as well as large Magnetic Reynolds number. Figures. 14 and 15 depict the growth rate as a function of wave number for small ($S \ll 1$) and large ($S \gg 1$) magnetic pressure number. It is observed from figures that the flow becomes stable in both cases.

The growth rate is shown in Figure. 16 as a function of wave number. It is found from the figure that the flow field is stable for smaller values of Brunt-Vaisala frequency and becomes unstable for larger Brunt-Vaisala frequency. Figure. 17 gives the growth rate vs wave number for different l . It is seen that the fluid becomes unstable with the increase in l . The growth rate as a function of wave number is shown through Figures. 18 and 19 for n and Ri . It is found

from Figure. 18 that there exists infinite number of normal modes for the given system. From Figure. 19, it is evident that increase in Ri stabilizes the fluid flow.

Figure. 20 shows the variation of growth rate as a function of Rm for various k . It is observed that increase in k depreciates the growth rate thereby stabilize the system. Figure. 21 depicts the growth rate interms of Magnetic pressure number for different k . It is noticed that increase in k declines the growth rate and therefore the system becomes stable. Figures (22) – (25) show the velocity profile for various non dimensional parameters. It is observed that the velocity profile increases with the increase in k and l when $\lambda > 0$. Velocity profile decreases with the increase in k and increases with the increase in Ri when $\lambda < 0$.

5. CONCLUSION

We have analyzed in this work the effect of magnetic field on the linear stability of an idealized stratified shear flow using series expansion method. Here we have discussed different cases and established the conditions for stability. Analysis is made using the normal mode approach to study the stability of fluid flow and the analysis is restricted to long wave approximation. The behavior of various nondimensional numbers like Magnetic Pressure Number, Magnetic Reynolds Number, longitudinal wave number, transverse wave number, Brunt- Vaisala frequency and Richardson number on the stability of parallel shear flow confined between the plates $z = \pm L$. From the results obtained, it is concluded that

- Richardson number plays a significant role in the stability of parallel stratified shear flows.
- Increase in wave number increases the growth rate for varying Magnetic Pressure Number and Magnetic Reynolds Number when $\lambda > 0$ thereby destabilizes the flow.
- Increase in transverse wave number destabilizes the fluid flow.
- With the increase in Richardson number the flow becomes unstable ($\lambda > 0$)
- The flow becomes unstable with the increase in wave number as Magnetic Reynolds Number increases.
- As Magnetic Reynolds Number increases, the flow is unstable for increase in Richardson number and Magnetic Pressure Number.
- As Brunt – Vaisala frequency increases there exists a stable fluid flow.
- Increase in Magnetic Reynolds Number, Magnetic Pressure Number and Richardson Number stabilize the fluid flow with the increase in wave number when $\lambda < 0$.
- Increase in Brunt – Vaisala frequency and transverse wave number results in instability of the flow region.
- Growth rate decreases for varying wave number and thereby stabilizes the flow with the increase in Magnetic Reynolds Number and Magnetic Pressure Number ($\lambda < 0$).

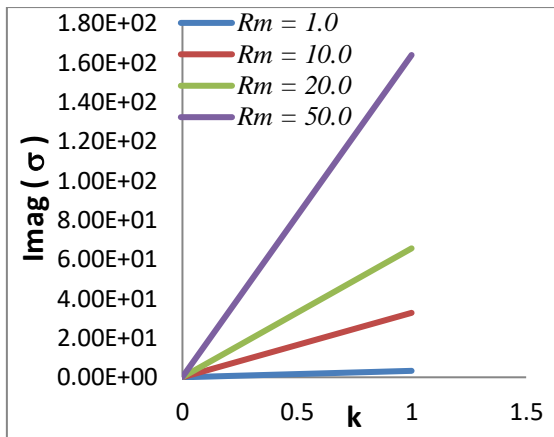


Figure 2 Growth rate vs wave number for various Rm

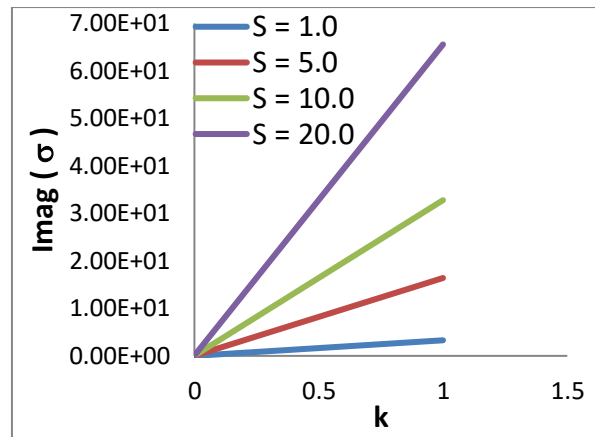


Figure 3 Growth rate vs wave number for various S

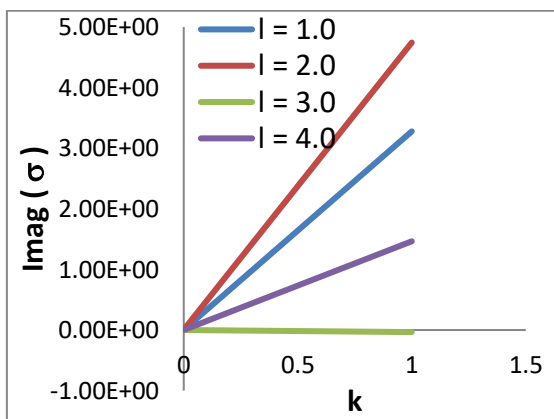


Figure 4 Growth rate vs wave number for various l

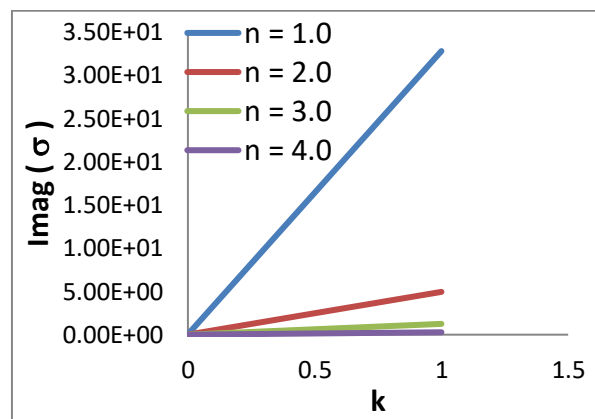


Figure 5 Growth rate vs wave number for various n

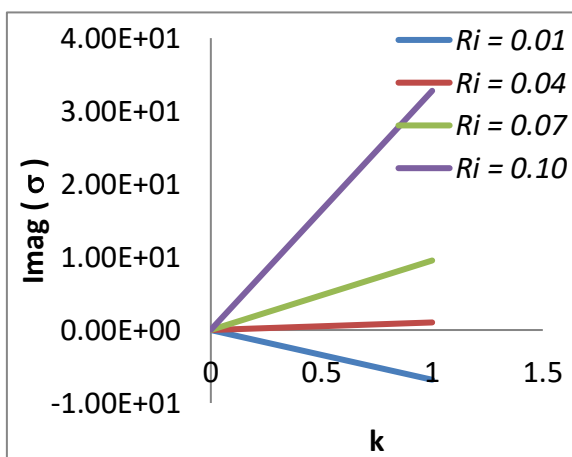


Figure 6 Growth rate vs wave number Reynolds for various Ri

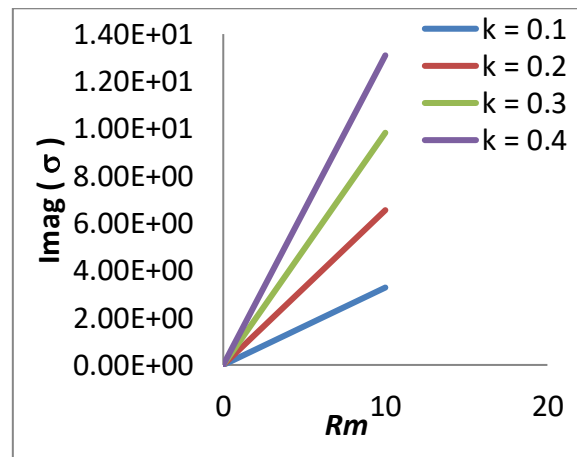


Figure 7 Growth rate vs Magnetic Number for various k

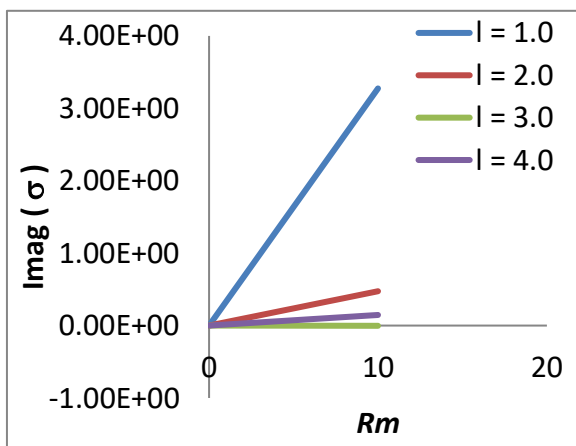


Figure 8 Growth rate vs Magnetic Reynolds Number for various l

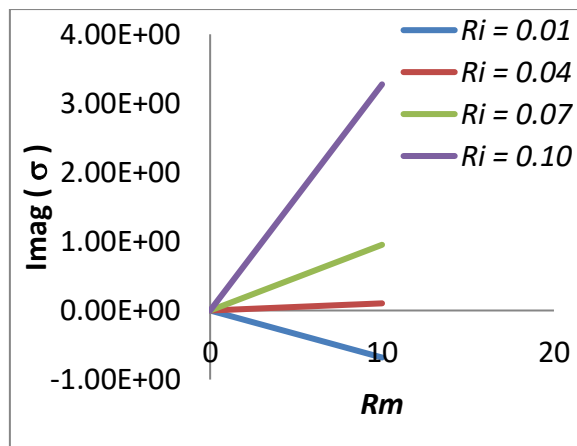


Figure 9 Growth rate vs Magnetic Reynolds Number for various Ri

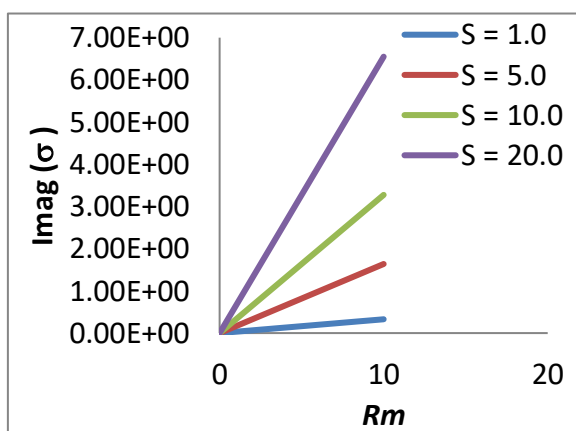


Figure 10 Growth rate vs Magnetic Reynolds Number for various S

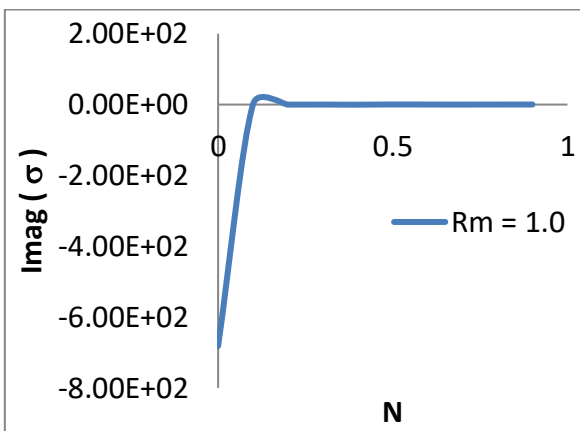


Figure 11 Growth rate vs Brunt – Vaisala frequency

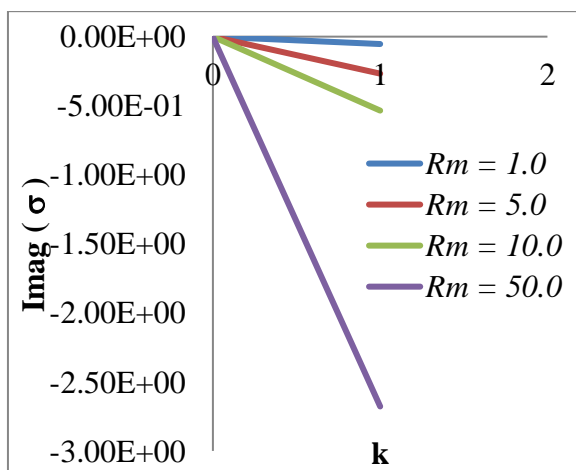


Figure 12 Growth rate vs wave number for various Rm

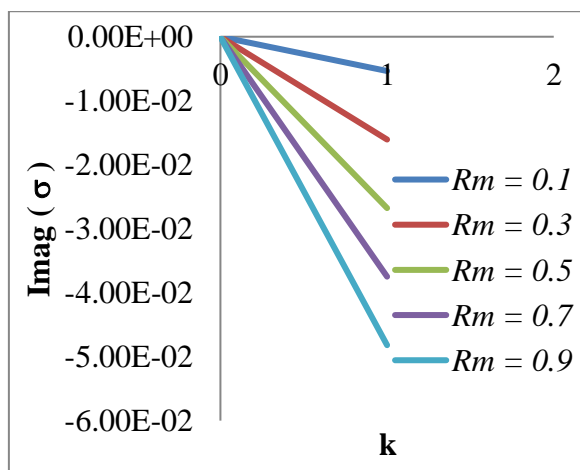


Figure 13 Growth rate vs wave number for various Rm ($Rm \ll 1$)

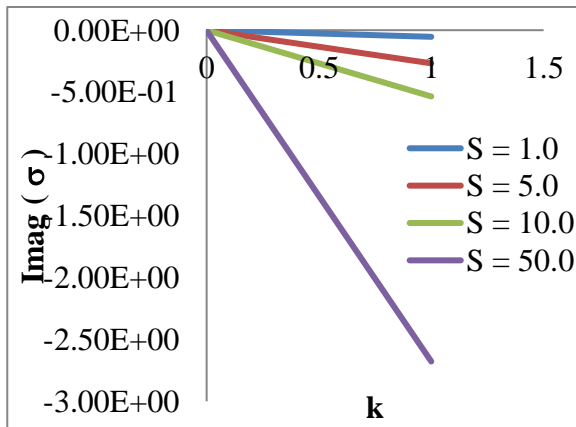


Figure 14 Growth rate vs wave number for various S

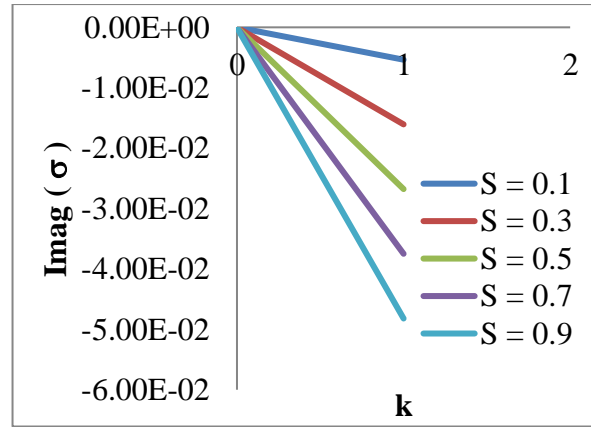


Figure 15 Growth rate vs wave number for various S ($S \ll 1$)

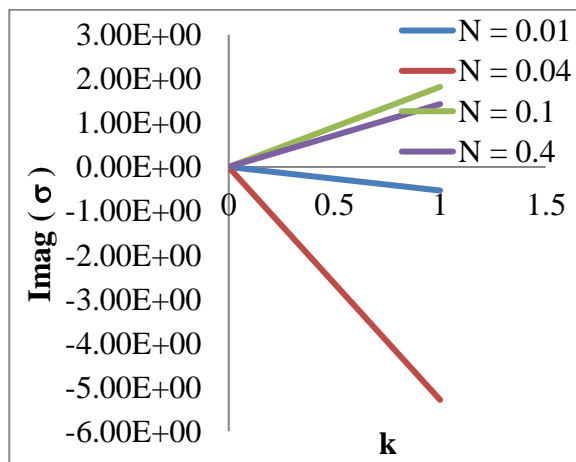


Figure 16 Growth rate vs wave number for various N

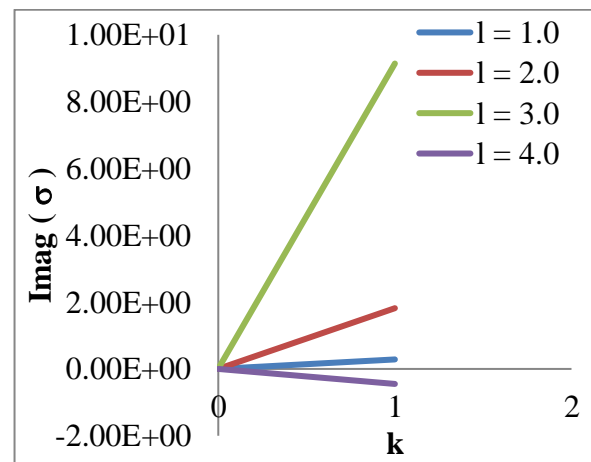


Figure 17 Growth rate vs wave number for various l

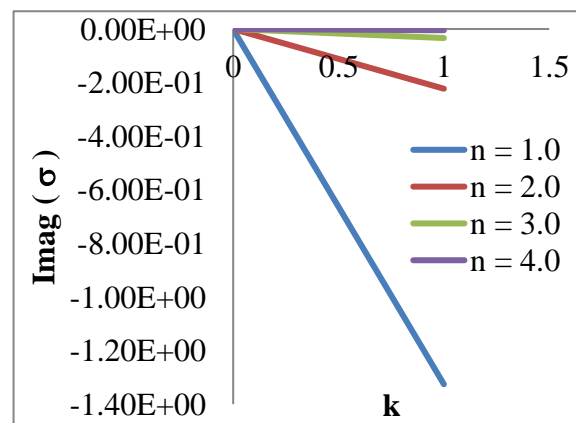


Figure 18 Growth rate vs wave number for various n

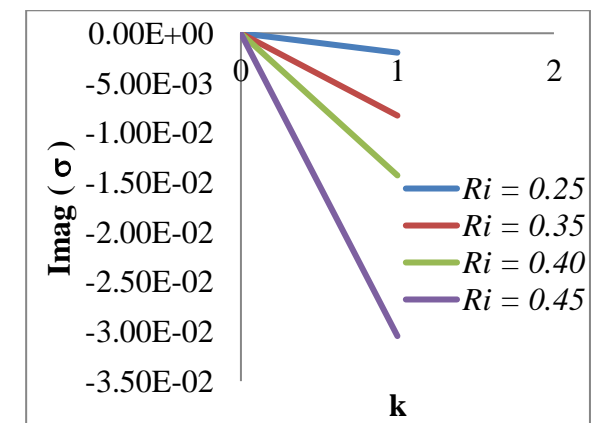


Figure 19 Growth rate vs wave number for various Ri

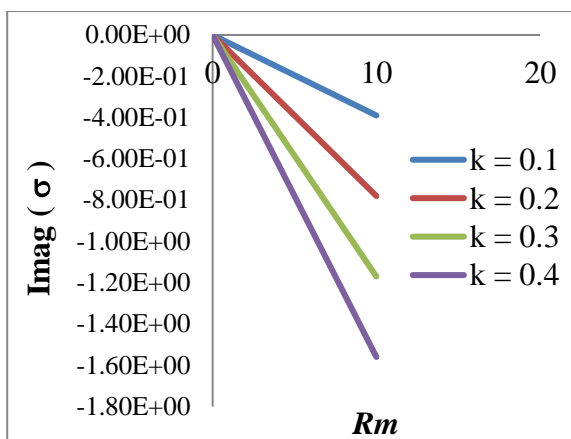


Figure 20 Growth rate vs Magnetic Reynolds Number for various k

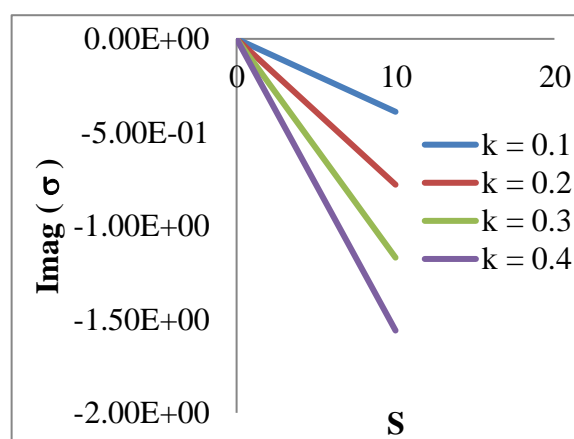


Figure 21 Growth rate vs Magnetic Pressure Number for various S

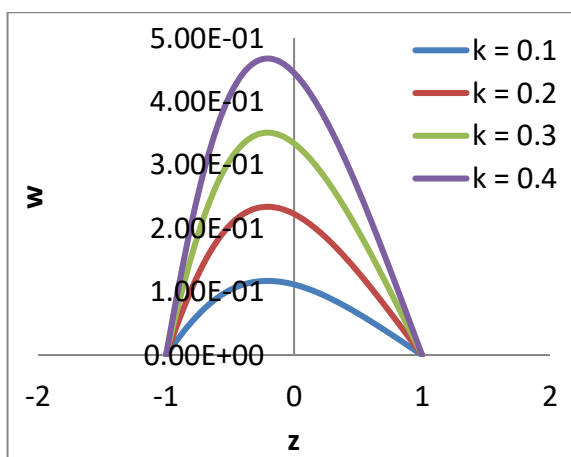


Figure 22 Velocity profile for various k ($\lambda > 0$)

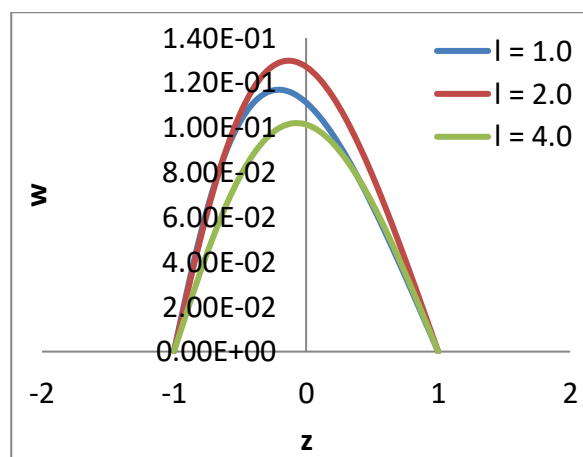


Figure 23 Velocity profile for various k ($\lambda > 0$)

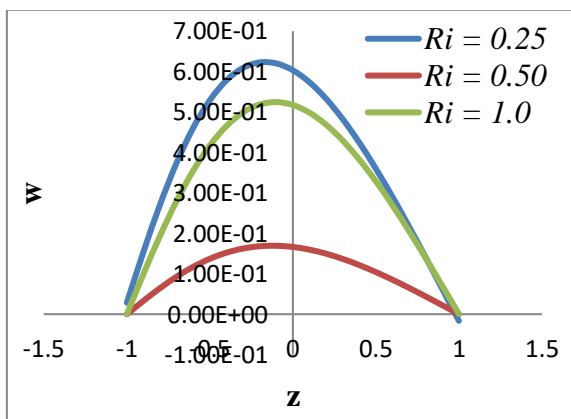


Figure 24 Velocity profile for various k ($\lambda < 0$)

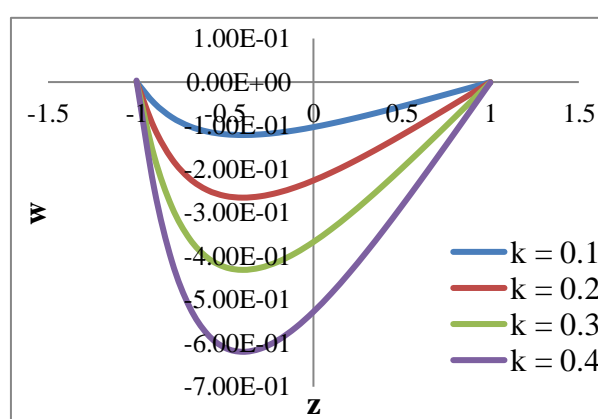


Figure 25 Velocity profile for various k ($\lambda < 0$)

REFERENCES

- [1] Agrawal S.C and Agrawal G.S., Hydromagnetic stability of heterogeneous shear flow, Journal of the Physical Society of Japan, 27, 1969, pp. 218-223.
- [2] Barston E. M., on the linear stability of inviscid, incompressible plane parallel flow, Journal of Fluid Dynamics, 233, 1991, pp. 157-163.

- [3] Collyer M. R., The stability of stratified shear flows, *Journal of Fluid Mechanics*, 42(2), 1970, pp. 367 – 377.
- [4] Drazin P G and Howard L N., Hydrodynamic stability of parallel flow of inviscid fluid, *Advances in Applied Mechanics*, 9, 1966, pp. 1-89.
- [5] Drazin P G and Reid W H., *Hydrodynamic Stability*, Cambridge University Press, 1981.
- [6] Drazin P G., Stability of parallel flow in a parallel magnetic field at small magnetic Reynolds numbers, *Journal of Fluid mechanics*, 8(1), 1960, pp. 130-142.
- [7] Goldstein S., On the stability of superposed streams of fluids of different densities, *Proceedings of Royal society of London A.*, 132, 1931, pp. 524-548.
- [8] Hirota M and Morrison P J., Stability boundaries and sufficient stability conditions for stably, stratified monotonic shear flows, *Physics Letters A*, 380, 2016, pp. 1856 - 1860.
- [9] Kent A., Instability of laminar flow of a perfect Magnetofluid, *Physics of Fluids*, 9, 1966, pp. 1286- 1289.
- [10] Kent A., Stability of laminar magneto fluid flow along a parallel magnetic field, *Journal of Plasma Physics*, 2(4), 1968, pp. 543 - 556.
- [11] Kochar G T and Jain R K., on Howard’s semi-circle theorem in hydromagnetics, *Journal of Physical Society of Japan*, 47(2), 1979, pp. 654 - 658.
- [12] Kuo H L., Dynamic instability of two dimensional non-divergent flows in a barotropic atmosphere, *Journal of Meteorology*, 6, 1949, pp. 105 – 122.
- [13] Padmini M and Subbiah M., Stability of non-parallel stratified shear flows, *International Journal of Pure and Applied Mathematics*, 26(5), 1995, pp. 471-483.
- [14] Rathy R K and Harikishan, Stability of hydromagnetic stratified shear flow, *Indian Journal of Pure and Applied Mathematics*, 12 (6), 1981, pp. 764 -768.
- [15] Reddy V R and Subbiah M., Stability of stratified shear flows in channels with variable cross sections, *Applied Mathematics and Mechanics*, 36(11), 2015, pp. 1459 – 1480.
- [16] Taylor G I., Effect of variation in density on the stability of superposed streams of fluids, *Proceedings of Royal Society of London A*, 132 (820), 1931, pp. 499 – 523.

Appendix

$$B = -(1 - \sigma_0)^{m_1 - m_2}$$

$$C_1 = \frac{N^2}{iN_0^2}$$

$$C_2 = \frac{B N^2}{iN_0^2}$$

$$C_3 = \frac{m_1 - 1}{i(1 + l^2)}$$

$$C_4 = \frac{B(m_2 - 1)}{i(1 + l^2)}$$

$$C_5 = -lC_3$$

$$C_6 = -lC_4$$

$$C_7 = -C_3 + i$$

$$C_{33} = C_{17}(C_{19}^{m_1+1}C_{20}^{m_2} - C_{20}^{m_1+1}C_{19}^{m_2})$$

$$C_{18}(C_{19}^{m_2+1}C_{20}^{m_2} - C_{20}^{m_2+1}C_{19}^{m_2})$$

$$C_{34} = \frac{C_{15}C_{31} + C_{16}C_{32}}{C_{30}}$$

$$C_{35} = \frac{C_{21}C_{31} + C_{23}C_{31}}{C_{30}}$$

$$C_{36} = \frac{C_{33}}{C_{30}}$$

$$C_{37} = C_{27}C_{19}^{m_1} + C_{34}C_{19}^{m_2} - C_{15}C_{19}^{m_1-1} - C_{16}C_{19}^{m_2-1}$$

$$C_{38} = C_{28}C_{19}^{m_1} + C_{35}C_{19}^{m_2} - C_{23}C_{19}^{m_1-1} - C_{24}C_{19}^{m_2-1}$$

$$C_{39} = C_{29}C_{19}^{m_1} + C_{36}C_{19}^{m_2} - C_{17}C_{19}^{m_1+1} - C_{18}C_{19}^{m_2+1}$$

$$\begin{aligned}
 C_8 &= -C_4 + iB & k &= \sqrt{p-1} \\
 C_9 &= \frac{-iH_0(1+l)}{(m_1+1)(m_1+2)} & F &= (1-\sigma_0)^{\frac{1}{2}} \sin(k \log(1-\sigma_0)) \\
 C_{10} &= \frac{-iH_0(1+l)}{(m_2+1)(m_2+2)} & C_{40} &= \frac{-iH_0(1+l)(-16k^2 - 64kF + 60)}{(4k^2+9)(4k^2+25)} \\
 C_{11} &= \frac{-iH_0(1+l)C_7}{m_1(m_1+1)} & C_{41} &= \frac{-iH_0(1+l)(-16k^2F + 64k + 60F)}{(4k^2+9)(4k^2+25)} \\
 C_{12} &= \frac{-iH_0(1+l)C_8}{m_2(m_2+1)} & C_{42} &= \frac{H_0l(-16k^3F + 40k^2 + 28kF - 6)}{(4k^2+1)(4k^2+9)} \\
 C_{13} &= \frac{-iH_0(1+l)C_5}{m_1(m_1+1)} & C_{43} &= \frac{H_0l(16k^3 + 40k^2F - 28k - 6F)}{(4k^2+1)(4k^2+9)} \\
 C_{14} &= \frac{-iH_0(1+l)C_6}{m_2(m_2+1)} & C_{44} &= \frac{-H_0(1+l) \left(\begin{matrix} 32l^2kF - 12l^2 - 24k^2 \\ +16k^2l^2 - 16k^3F + 4kF - 6 \end{matrix} \right)}{(1+l^2)(4k^2+1)(4k^2+9)} \\
 p &= \frac{Ri N^2}{N_0^2} (1+l^2) & C_{45} &= \frac{-H_0(1+l) \left(\begin{matrix} 32l^2k - 12l^2F - 24k^2D \\ +16k^2l^2F - 16k^3 + 4k - 6F \end{matrix} \right)}{(1+l^2)(4k^2+1)(4k^2+9)} \\
 C_{15} &= \frac{i(1+l^2)C_1}{(m_1-1)^2 - (m_1-1) + p} & C_{46} &= m^2 - \frac{3}{4} - p \\
 C_{16} &= \frac{i(1+l^2)C_2}{(m_2-1)^2 - (m_2-1) + p} & C_{47} &= (5p-3)(C_{46} - 2kF) \frac{(1-\sigma_0)^{-\frac{1}{2}}}{4k^2 + C_{46}} \\
 C_{17} &= \frac{iH_0(1+l)C_{11}(m_1+1)}{(m_1+1)^2 - (m_1+1) + p} & C_{48} &= (C_{46} + 5kF) \frac{iH_0^2(1+l^2)(1-\sigma_0)^{\frac{3}{2}}}{25k^2 + C_{46}} \\
 C_{18} &= \frac{iH_0(1+l)C_{12}(m_1+1)}{(m_2+1)^2 - (m_2+1) + p} & C_{49} &= (5p-3)(C_{46} + 2k) \frac{(1-\sigma_0)^{-\frac{1}{2}}}{4k^2 + C_{46}} \\
 C_{19} &= 1 - \sigma_0 & C_{50} &= (C_{46}F - 5k) \frac{iH_0^2(1+l^2)(1-\sigma_0)^{\frac{3}{2}}}{25k^2 + C_{46}} \\
 C_{20} &= -1 - \sigma_0 & C_{51} &= (5p-3)(C_{46} - 2kF) \frac{(-1-\sigma_0)^{-\frac{1}{2}}}{4k^2 + C_{46}} \\
 C_{21} &= m_1(m_1-1) & C_{52} &= (C_{46} + 5kF) \frac{iH_0^2(1+l^2)(-1-\sigma_0)^{\frac{3}{2}}}{25k^2 + C_{46}} \\
 C_{22} &= C_{19}^{m_1-1} C_{20}^{m_1} - C_{20}^{m_1-1} C_{19}^{m_1} & C_{53} &= (5p-3)(C_{46} + 2k) \frac{(-1-\sigma_0)^{-\frac{1}{2}}}{4k^2 + C_{46}} \\
 C_{23} &= m_2(m_2-1) & C_{54} &= (C_{46}F - 5k) \frac{iH_0^2(1+l^2)(-1-\sigma_0)^{\frac{3}{2}}}{25k^2 + C_{46}} \\
 C_{24} &= C_{19}^{m_2-1} C_{20}^{m_1} - C_{20}^{m_2-1} C_{19}^{m_1} & C_{55} &= (1-\sigma_0)^{\frac{1}{2}}(-1-\sigma_0)^{\frac{1}{2}} \\
 & & & (\sin(k \log(1-\sigma_0)) - \cos(k \log(-1-\sigma_0)))
 \end{aligned}$$

$$C_{25} = C_{17}(C_{19}^{m_1+1}C_{20}^{m_1} - C_{20}^{m_1+1}C_{19}^{m_1}) + C_{18}(C_{19}^{m_2+1}C_{20}^{m_1} - C_{20}^{m_2+1}C_{19}^{m_1})$$

$$C_{26} = C_{19}^{m_2}C_{20}^{m_1} - C_{20}^{m_2}C_{19}^{m_1}$$

$$C_{27} = \frac{C_{15}C_{22} + C_{16}C_{24}}{C_{26}}$$

$$C_{28} = \frac{C_{21}C_{22} + C_{23}C_{24}}{C_{26}}$$

$$C_{29} = \frac{C_{25}}{C_{26}}$$

$$C_{30} = C_{19}^{m_1}C_{20}^{m_2} - C_{20}^{m_1}C_{19}^{m_2}$$

$$C_{31} = C_{19}^{m_1-1}C_{20}^{m_2} - C_{20}^{m_1-1}C_{19}^{m_2}$$

$$C_{32} = C_{19}^{m_2-1}C_{20}^{m_2} - C_{20}^{m_2-1}C_{19}^{m_2}$$

$$C_{56} = C_{49}(-1 - \sigma_0)^{\frac{1}{2}}\sin(k\log(1 - \sigma_0))\cos(k\log(-1 - \sigma_0))$$

$$-C_{53}(1 - \sigma_0)^{\frac{1}{2}}\sin(k\log(-1 - \sigma_0))\cos(k\log(1 - \sigma_0))$$

$$C_{57} = C_{50}(-1 - \sigma_0)^{\frac{1}{2}}\sin(k\log(1 - \sigma_0))\cos(k\log(-1 - \sigma_0))$$

$$-C_{54}(1 - \sigma_0)^{\frac{1}{2}}\sin(k\log(-1 - \sigma_0))\cos(k\log(1 - \sigma_0))$$

$$C_{58} = (1 - \sigma_0)^{\frac{1}{2}}\cos(k\log(1 - \sigma_0))$$

$$C_{59} = C_{47}\cos(k\log(1 - \sigma_0))$$

$$\frac{C_{56}(1 - \sigma_0)^{\frac{1}{2}}\sin(k\log(1 - \sigma_0))}{C_{55}}$$

$$+C_{49}\sin(k\log(1 - \sigma_0))$$

$$C_{60} = C_{48}\cos(k\log(1 - \sigma_0))$$

$$\frac{C_{57}(1 - \sigma_0)^{\frac{1}{2}}\sin(k\log(1 - \sigma_0))}{C_{55}}$$

$$+C_{50}\sin(k\log(1 - \sigma_0))$$

$$C_{61} = C_{47}\cos(k\log(1 - \sigma_0))$$

$$+C_{49}\sin(k\log(1 - \sigma_0))$$

$$\frac{C_{59}(1 - \sigma_0)^{\frac{1}{2}}\sin(k\log(1 - \sigma_0))}{C_{58}}$$

$$\frac{C_{56}(1 - \sigma_0)^{\frac{1}{2}}\sin(k\log(1 - \sigma_0))}{C_{55}}$$

$$C_{62} = C_{48}\cos(k\log(1 - \sigma_0))$$

$$+C_{50}\sin(k\log(1 - \sigma_0))$$

$$\frac{C_{60}(1 - \sigma_0)^{\frac{1}{2}}\sin(k\log(1 - \sigma_0))}{C_{58}}$$

$$\frac{C_{57}(1 - \sigma_0)^{\frac{1}{2}}\sin(k\log(1 - \sigma_0))}{C_{55}}$$